

Experimental probe for the production of ^{97}Ru from the $^7\text{Li} + ^{93}\text{Nb}$ reaction: A study of precompound emissions

Deepak Kumar and Moumita Maiti*

Department of Physics, Indian Institute of Technology Roorkee, Roorkee 247667, Uttarakhand, India

Susanta Lahiri

Chemical Sciences Division, Saha Institute of Nuclear Physics, 1/AF Bidhannagar, Kolkata 700064, India

(Received 3 August 2016; published 10 October 2016)

Background: Interaction of weakly bound heavy ions with an intermediate or heavy target is not yet understood completely due to the scarcity of experimental data. In order to develop a clear understanding of breakup fusion or preequilibrium emission even in the low energy range, 3–10 MeV/nucleon, more experimental investigations are necessary.

Purpose: We aim to study the reaction mechanisms involved in the weakly bound heavy-ion induced reaction $^7\text{Li} + ^{93}\text{Nb}$ at low energies by measuring the production cross sections of the residual radionuclides.

Method: Natural niobium (^{93}Nb) foil, backed by an aluminum (Al) catcher, arranged in a stack was bombarded by ^7Li ions of 20–45 MeV energy. Activity of the residues produced in each ^{93}Nb target was measured by off line γ -ray spectrometry after the end of bombardment (EOB) and cross sections were calculated. Experimental cross sections were compared with those computed using compound and precompound models.

Results: In general, measured excitation functions of all residues produced in the $^7\text{Li} + ^{93}\text{Nb}$ reaction showed good agreement with the model calculations based on the Hauser-Feshbach formalism and the exciton model for compound and precompound processes, respectively. Significant preequilibrium emission of neutrons was observed at the relatively high energy tail of the excitation function of ^{97}Ru .

Conclusions: Preequilibrium processes played an important role in the enhancement of the cross section in the xn reaction channel over the compound reaction mechanism at higher energies for the $^7\text{Li} + ^{93}\text{Nb}$ reaction. Additionally, indirect evidence of incomplete or breakup fusion was also perceived.

DOI: [10.1103/PhysRevC.94.044603](https://doi.org/10.1103/PhysRevC.94.044603)

I. INTRODUCTION

The study of interactions of weakly bound light heavy-ion induced reactions with intermediate or heavy nuclei at low projectile energies was started about a half century ago. However, complete understanding of the mechanism of heavy-ion reactions is still lacking compared to light-ion reactions, hence it has been a subject of great interest for many years [1–3]. Investigations of fusion reactions involving either weakly bound stable nuclei or unstable nuclei far from the stability region have become important to understand complete fusion (CF) and incomplete fusion (ICF) reactions, nucleon transfer reactions, preequilibrium (PEQ) reactions, and quasifission because of low nucleon (cluster) separation energies [4–8]. In addition to that, fusion with weakly bound nuclei is also an important tool to study astrophysical reactions, such as in understanding nucleosynthesis processes and in studying nuclei near the drip line [9]. Investigations with weakly bound unstable nuclei are being carried out at radioactive ion beam (RIB) facilities which usually deliver low intensity beams. The study of reactions induced by stable nuclei is therefore important, as they produce good quality statistical data, which aids in understanding reaction dynamics and comparing reaction quantities obtained by weakly bound unstable projectiles.

Studies of PEQ processes over the compound nuclear reaction are especially important, as the particles that are emitted prior to statistical equilibrium provide necessary information about the dynamics of the excited composite system and the mechanism by which it attains statistical equilibrium. A substantial signature of the PEQ process has been witnessed in the high energy tail of excitation functions of light- and heavy-ion induced reactions. However, besides compound and precompound processes, ICF also starts to compete in heavy-ion induced reaction at relatively high energy (10–25 MeV/nucleon) [10–14]. Birattari *et al.* [10], Cavinato *et al.* [11], and Vergani *et al.* [12] experimented on the ^{12}C and/or ^{16}O induced reactions on different targets and observed PEQ emission of nucleons during the thermalization of the compound system. Moreover, the PEQ process was also observed at a relatively low energy, ~ 4 –8 MeV/nucleon, where the pure evaporation process is dominant. PEQ emission of α particles was reported by Amorini *et al.* [15] in complete and incomplete fusion reactions in the $^{12}\text{C} + ^{64}\text{Ni}$ reaction at 8 MeV/nucleon. Sharma *et al.* [16] analyzed the PEQ emission of neutrons from ^{12}C and ^{16}O induced reaction on ^{128}Te , ^{169}Tm , ^{159}Tb , and ^{181}Ta targets at 4–7 MeV/nucleon. More experimental investigations near the barrier are necessary to draw specific conclusions and to develop a sophisticated theory for PEQ and CF-ICF processes in weakly bound nuclear reactions.

Among the ruthenium isotopes, neutron deficient ^{97}Ru has the potential, owing to its low lying intense γ lines [215.70 keV (85.62%) and 324.49 keV (10.79%) energy] and moderate half-life (2.83 d), to be used in several applications. The

*Corresponding author: moumifph@iitr.ac.in;
moumifph@gmail.com

ability to form wide varieties of chemical complexes made ^{97}Ru lucrative to the nuclear medicine community. Moreover it can be produced in the no-carrier-added state which is the prerequisite of such applications [17].

Its production by neutron or light-ion induced reactions (such as with p , α , or ^3He) was investigated earlier by several groups [18–23]. ^{97}Ru was prepared from high energy proton spallation (200 or 67.5 MeV) on a natural rhodium (^{103}Rh) target through the $^{103}\text{Rh}(p, 2p5n)^{97}\text{Ru}$ reaction [18,19] along with the radionuclides of Tc, Rh, and Pd as impurities. Enormous production of ^{97}Ru was reported from a 50 MeV proton induced reaction on the radioactive target ^{99}Tc [20]. Besides protons, α -particle and ^3He induced reactions on natural molybdenum targets also led to the production of ^{97}Ru via $^{\text{nat}}\text{Mo}(^4\text{He}, xn)^{97}\text{Ru}$ and $^{\text{nat}}\text{Mo}(^3\text{He}, xn)^{97}\text{Ru}$ reactions [21–23], respectively, along with Tc and Ru contaminants. Although enriched ^{96}Ru is expensive, the easiest way to produce ^{97}Ru is by the thermal neutron capture reaction, $^{96}\text{Ru}(n, \gamma)^{97}\text{Ru}$, but this leads to the low specific activity of ^{97}Ru .

Recently, heavy-ion (^7Li , ^{12}C) induced productions of ^{97}Ru on natural Nb and Y were investigated by Maiti *et al.* and a subsequent chemical separation of ^{97}Ru from the target matrix was developed [24–26]. In this article, we have made an effort to study (i) the relevance of the PEQ plus CF-ICF mechanism in a light heavy-ion induced reaction, $^7\text{Li} + ^{93}\text{Nb}$, in the low energy range of 20–42 MeV, and (ii) the production of ^{97}Ru along with the coproduced radionuclides at various impinging energies, which is essential to determine the optimized production parameters for ^{97}Ru .

The experimental procedure and a brief description of the nuclear model calculations are presented in Secs. II and III, respectively. Section IV discusses the results of the present study and Sec. V concludes the report.

II. EXPERIMENT

A. Measurement of activity

A ^7Li -ion beam up to 45 MeV energy obtained from BARC-TIFR Pelletron Accelerator facility, Mumbai, India, was used for the experiment. Spectroscopically pure (99.99%) natural niobium (^{93}Nb) was procured from Alfa Aesar and self supporting Nb foils of 2.3–3.2 mg/cm² were prepared by proper rolling. The niobium and aluminum (^{27}Al) foils were mounted on an aluminum ring of 12 mm inner and 22 mm outer diameter with 0.5 mm thickness. The $^7\text{Li}^{3+}$ -ion beam was allowed to impinge on niobium targets backed by Al foils of ~ 1.5 mg/cm² arranged in a stack. A total of six such Nb-Al foil stacks were irradiated individually varying the incident energy of $^7\text{Li}^{3+}$ ions with a slight overlap between them. The total charge of each irradiation was measured by an electron-suppressed Faraday cup placed at the rear of the target assembly. Use of Al foil served the purpose of an energy degrader as well as catcher for recoils, if any, in the beam direction. The large area of the catcher foils ensured the complete collection of recoiled evaporation residues. The duration of the irradiation time was chosen according to the beam intensity and half-lives of the product radionuclides.

Energy degradation in each foil was estimated by the code Stopping and Range of Ions in Matter (SRIM) [27]. The projectile energy at a target is estimated by averaging the incident and outgoing beam energies.

After the end of bombardment (EOB), target ^{93}Nb and catcher ^{27}Al foils were assayed using off line γ spectrometry in a regular time interval for a sufficient time to measure the activity of the residues with the help of a Falcon 5000 broad energy germanium (BEGe) based detector, having enhanced efficiency and resolution at low energy while still preserving good efficiencies at high energies, coupled with a PC operating with GENIE-2K software (Canberra). The detector was calibrated using the standard sources, ^{152}Eu (13.506 a), ^{137}Cs (30.08 a), ^{60}Co (5.27 a), ^{133}Ba (10.51 a), of known activity. The energy resolution of the detector was ≤ 2.0 keV at 1332 keV energy. The background subtracted peak area count corresponding to a particular γ -ray energy is the measure of yield of an evaporation residue [28].

The cross section of the n th evaporation residue, $\sigma_n(E)$ at an incident energy E is calculated from the equation

$$\sigma_n(E) = \frac{Y_n}{I_{pro} N_{tg} x_{tg} (1 - e^{-\lambda_n T})}. \quad (1)$$

The yield (Y_n) of an evaporation residue n at the EOB was calculated from the equation

$$Y_n = \frac{C(t)}{\varepsilon_n^\gamma I_n^m} e^{\lambda_n \tau}, \quad (2)$$

where $C(t)$ is the count rate (counts per second), ε_n^γ and I_n^m are the detection efficiency and branching intensity of the characteristic γ ray of the evaporation residue, the decay constant is λ^n , and the cooling time is τ . I_{pro} is the beam intensity of the projectile ions, N_{tg} and x_{tg} are the number of target nuclei per unit volume and target thickness, respectively, and T is the duration of irradiation [29,30]. The nuclear spectroscopic data used to calculate the production cross sections of the evaporation residue are enlisted in Table I [31].

B. Estimation of uncertainties

Uncertainties in the cross-section measurement may come from the following: (i) inaccuracy in efficiency calibration of the detector $\sim 2\%$; (ii) nonuniformity of samples and measurement of their thicknesses in atoms/cm² may cause error $\sim 5\%$; (iii) uncertainty in the beam current measurement was $\sim 5\%$; (iv) error propagated to the cross-section measurement from the counting statistics, which is negligible in this case; and (v) error in the estimation of beam energy due to the degradation of energy while traversing through the successive target foils; however, energy straggling effects are expected to be very small and are neglected in the calculation [32,33]. The total uncertainty associated with the cross-section measurement was determined considering all those factors and the data have up to 95% confidence level.

III. THEORETICAL CALCULATION

Nuclear reactions can be broadly classified into three reaction mechanisms: direct (DIR), preequilibrium (PEQ),

TABLE I. Spectroscopic data [31] of the residual radionuclides and list of contributing reactions.

Nuclides (J^π)	Half-life	Decay mode (%)	E_γ (keV) [I_γ (%)]	Reactions	E_{th} (MeV) ^a
⁹⁷ Ru(5/2 ⁺)	2.83 d	ϵ (100)	215.7 [85.6] 324.5 [10.8]	⁹³ Nb(⁷ Li, 3n)	11.2
⁹⁵ Ru(5/2 ⁺)	1.64 h	ϵ (100)	336.4 [70.2] 626.6 [17.8]	⁹³ Nb(⁷ Li, 5n)	31.4
⁹⁶ Tc(7 ⁺)	4.28 d	ϵ (100)	778.2 [99.8] 812.5 [82] 849.9 [98]	⁹³ Nb(⁷ Li, p3n) ⁹³ Nb(⁷ Li, d2n) ⁹³ Nb(⁷ Li, tn) ⁹³ Nb(⁷ Li, t) ⁹⁷ Tc \rightarrow ⁹⁶ Tc + n	19.3 16.9 10.2 39.6
⁹⁵ Tc(9/2 ⁺)	20 h	ϵ (100)	765.8 [93.8]	⁹³ Nb(α , n) - ICF ⁹³ Nb(⁷ Li, p4n) ⁹³ Nb(⁷ Li, d2n)	7.3 27.8 25.4
^{93m} Mo(21/2 ⁺)	6.85 h	IT ^b (99.88) ϵ (0.12)	263.1 [56.7] 684.7 [99.7]	⁹³ Nb(⁷ Li, α 3n) ⁹³ Nb(⁷ Li, 2p5n)	13.1 43.5

^a E_{th} represents threshold energy.

^bIT represents isomeric transition.

equilibrium or evaporation (EQ). Production of a residual nucleus in a nuclear reaction is the contribution from all three types. In this endeavor, an effort has been made to explain the measured cross-section data of the residues produced in the ⁷Li + ⁹³Nb reaction in terms of PEQ and EQ reactions in the 20–45 MeV energy range using nuclear reaction model codes PACE4 [34], ALICE91 [35,36], and EMPIRE3.2 [37]. In general, contribution of DIR reaction is not expected at low incident energies.

A. PACE4

PACE4 is based on the Hauser-Feshbach formalism which follows the correct procedure of angular momentum coupling at each stage of deexcitation of an excited nuclei. For heavy projectiles, the fusion cross section and initial spin distribution are calculated by the Bass model [38] while the optical model is used for light ions. However, heavy-ion fusion near and below the barrier and reactions induced by very heavy beams cannot be accurately determined by the Bass model. The transmission coefficients for light particle emission are created by the optical model calculations where all the optical model parameters are taken from Ref. [39]. The shift in the Coulomb barrier during deexcitation is accounted for by calculating the transmission coefficients at an effective energy determined by the shift. Fission is considered as a decay mode, and the fission barrier can be changed accordingly in the program. The Gilbert-Cameron level density is used in the calculation, with level density parameter $a = A/10$, where A is the mass number of compound nucleus. The a ratio, a_f/a_n , is taken as unity. The modified rotating liquid drop barrier of Sierk is adopted. A nonstatistical yrast cascade γ decay chain is artificially incorporated to simulate gamma multiplicity.

B. ALICE91

ALICE91 has been used to study EQ and PEQ emission of particles in the ⁷Li + ⁹³Nb reaction. A hybrid or geometry-dependent hybrid model [40] computes the PEQ emission of particles and the Weisskopf-Ewing model [41] accounts for the compound emission process. It does not account for the

direct reaction processes. In the hybrid model, emission of particles results from the two-body interaction process in an excited projectile-target composite system. Each stage of the relaxation process is specified by the exciton number (n_0) of excited particles, i.e., the sum of excited particles (p) and holes (h). The hybrid model uses the never-come-back approximation; i.e., in each two-body interaction, p-h pairs may either be created or redistribution of energy may take place among the excitons. It explicitly determines the PEQ emission energy distribution of the excited particles, which helps to estimate high energy emissions more accurately. Details of the hybrid model are available elsewhere [17,28]. The geometry-dependent hybrid model is selected for the calculation to include the nuclear surface effect. In ALICE91, light particles emissions (n , p , d , etc.) from an equilibrated nucleus are calculated up to 12 mass units wide and 10 charge units deep from the composite nucleus system. Fermi gas level density is used for the cross-section calculation with level density parameter $a = A/9$ MeV⁻¹. The optical model is used for the calculation of the inverse reaction cross section. The rotating finite-range fission barriers of Sierk have been selected. The total number of nucleons in the projectile has been chosen as the initial exciton number for the PEQ cross-section calculation.

C. EMPIRE3.2

EMPIRE3.2 code accounts all the three major nuclear reactions: EQ, PEQ, and DIR. For the compound reaction process, the detailed Hauser-Feshbach model, which follows the exact coupling of angular momentum and parity of emitted particles and residual nucleus, is used including width fluctuations and the optical model for fission. PEQ emission can be calculated either by quantum mechanical PEQ models (multi-step direct (MSD) or multi-step compound (MSC) mechanism [42]) or by phenomenological PEQ models (exciton model or hybrid Monte Carlo simulation [43]). A coupled-channels approach or distorted wave Born approximation (DWBA) [44,45] is used for the calculation of direct processes. The code can be applied to the calculation of neutron capture in the keV

region, as well as for heavy-ion induced reactions at several hundreds of MeV. A coupled-channels calculation (CCFUS) [46] is used for the heavy-ion fusion cross section. Nuclear masses, optical model parameters, ground state deformations, discrete levels and decay schemes, level densities, fission barriers, and γ -ray strength functions are internally provided by input library RIPL-3. In our calculation, the exciton model is used for the PEQ emission process and enhanced generalized superfluid model (EGSM) level density is used to consider the collective (rotational/vibrational) effect of nuclei on nuclear level density.

In the EGSM, the effect of superconducting pairing correlations, which strongly influence the nuclear level density at lower energy, is considered as a correlation function δ_0 . The EGSM is build on the Fermi gas model (FGM) level density in an adiabatic mode along with a collective enhancement factor which damps out with increasing excitation energy (E_x) and reduces to unity above a critical temperature (T_c); that is, it reduces naturally to the FGM above T_c . In this model, the critical level density parameter (a_c) is used below T_c , while the Ignatyuk empirical level density parameter, $a(E_x) = \tilde{a} [1 + (1 - e^{-\gamma_s U^*}) \delta S / U^*]$, is used above T_c , where parameters $\tilde{a} = 0.0748A$ and $\gamma_s = 0.5609A^{1/3}$ are the asymptotic value of the a parameter and the shell effects damping parameter, respectively. δS is the shell correction which fades out with increasing excitation energy (E_x) and $U^* = U - 0.1521a_c \delta_0^2$, is the effective energy above T_c , while, below T_c , U is used as effective energy, $U = E_x + n\delta_0$, where the correlation function is calculated as $\delta_0 = 12/\sqrt{A}$, and $n = 0, 1$, and 2 for odd-odd, odd- A , and even-even nuclei, respectively.

IV. DISCUSSION OF RESULTS

Analysis of the time resolved γ -ray spectra collected after EOB was carried out for each set of Nb-Al foils to identify the residual radionuclides produced in the ${}^7\text{Li} + {}^{93}\text{Nb}$ reaction at different incident energies. It ensured the production of ${}^{97}\text{Ru}$, ${}^{95}\text{Ru}$, ${}^{96}\text{Tc}$, ${}^{95}\text{Tc}$, and ${}^{93m}\text{Mo}$ in the target matrix. A typical γ -ray spectrum of the evaporation residues produced in the ${}^7\text{Li} + {}^{93}\text{Nb}$ reaction at 42 MeV incident energy collected 34 minutes after the EOB is presented in Fig. 1, showing characteristic γ rays. The possible reactions contributing to the production of the residues are listed in Table I along with the reaction thresholds. Measured cross sections of the evaporation residues at various energies are listed in Table II. Comparison between the experimental excitation functions of the residues and those theoretically computed using the nuclear reaction model codes PACE4 [34], ALICE91 [35,36], and EMPIRE3.2 [37] are shown in Figs. 2–6. Experimentally measured cross sections are shown by symbols with an error bar, while theoretical calculations are shown by curves.

Figure 2 shows the production cross sections of ${}^{97}\text{Ru}$ in the 20–45 MeV energy range. It is observed that, at low energies, experimental cross sections are well reproduced by all three theoretical calculations. However, in the higher energy region (~ 5 –7 MeV/nucleon) a clear deviation is observed between the measured cross sections and the PACE4 estimation, while ALICE91 and EMPIRE3.2 are in good agreement with the experimental data. The reason is that PACE4 computation

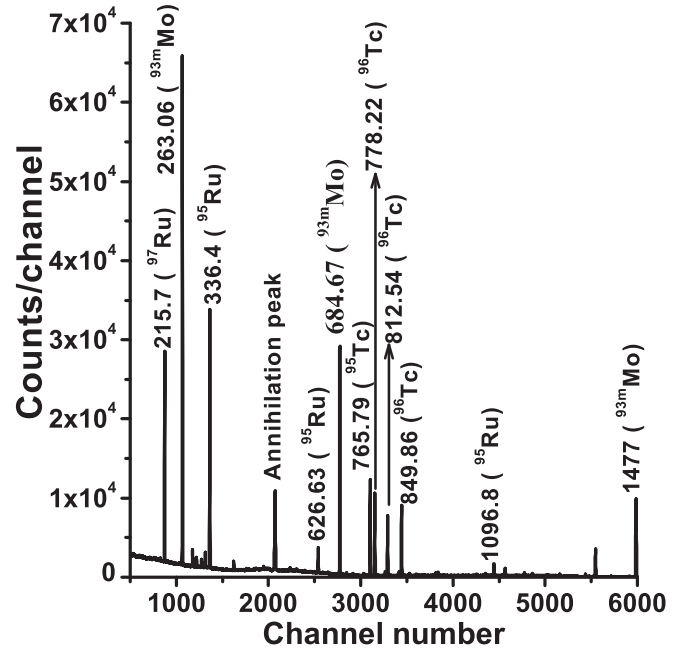


FIG. 1. γ -ray spectrum of ${}^7\text{Li}$ activated niobium foil collected 34 minutes after the EOB.

is based only on the compound nuclear model using the Hauser-Feshbach formalism, whereas ALICE91 and EMPIRE3.2 both considered PEQ as well as the compound nuclear model in the calculation. It is evident that significant PEQ emission occurs around the 5–7 MeV/nucleon energy region. A critical observation also shows that the EMPIRE3.2 prediction reproduced the experimental cross section more accurately than the ALICE91.

A comparison of measured and theoretical excitation functions of ${}^{95}\text{Ru}$ is shown in Fig. 3. Experimental data agree well with EMPIRE3.2 calculation throughout the measured energy range but PACE4 underpredicts the measured data below 42 MeV. This might be due to inclusion of the enhanced generalized superfluid model density in EMPIRE3.2, as it accounts for the collective (rotational/vibrational) effect of the nuclear level density which enhances the nuclear level density below the critical energy. ALICE91 overpredicts the data by about four times over the energy range studied. The PEQ emission is observed in the $3n$ reaction channel (Fig. 2) instead of the $5n$ reaction channel. It is anticipated that one PEQ neutron emission is more likely than two or more near the barrier energy, hence PEQ emission of one neutron from an excited composite nuclear system is possible even at low projectile energy.

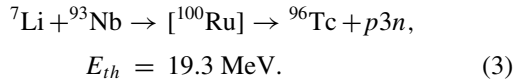
Figure 4 represents the excitation function of ${}^{96}\text{Tc}$ radionuclides in the 20–45 MeV energy interval. All three theoretical estimations reproduce the experimental data in the higher energy region but underpredict the cross sections at low energies. Besides complete fusion and the PEQ mechanism, the higher experimental cross sections of ${}^{96}\text{Tc}$ in the low energy region might be attributed to the incomplete fusion (ICF) process, which is likely to occur in the interaction of weakly bound projectile ${}^7\text{Li}$ with ${}^{93}\text{Nb}$. Thus ${}^{96}\text{Tc}$ might be

TABLE II. Cross section (mb) of residues at different incident energies.

Energy (MeV)	Cross section (mb)				
	^{97}Ru	^{95}Ru	^{96}Tc	^{95}Tc	^{93m}Mo
20.4	133.6 ± 14		9.7 ± 0.8		
22.6	320 ± 33.3		22.1 ± 1.8		
24.7	503.3 ± 52.1		34.6 ± 2.7		
25.7	547.3 ± 48.9		42 ± 2.9		
26.7	575.3 ± 59.6		42.5 ± 3.3		
27.9	530.3 ± 47.4		53.1 ± 3.4		
28.3	508.4 ± 45.5		36.9 ± 2.5	1.2 ± 0.2	
28.5	587.3 ± 52.7		55.6 ± 3.7	3.6 ± 0.4	0.2 ± 0.1
30.0	502.2 ± 44.9		79.8 ± 5.1	8.5 ± 0.8	1.8 ± 0.2
31.8	492.6 ± 44.1		74.3 ± 4.8	8 ± 0.8	1.6 ± 0.1
32.3	382.3 ± 34.2		107.5 ± 6.8	13 ± 1.2	6.1 ± 0.4
35.1	371.2 ± 33.4		146.4 ± 9.3	19.4 ± 1.8	12.3 ± 0.9
38.1	226.3 ± 20.4	2.3 ± 0.4	254.3 ± 16	37.8 ± 3.4	39.5 ± 2.6
39.5	173.4 ± 24	11 ± 1.8	339.9 ± 37.8	70.3 ± 13.5	65.6 ± 7.3
41.1	176.9 ± 24.5	29 ± 4.6	478.9 ± 53.2	131.5 ± 25.3	104.1 ± 11.6
41.5	126.6 ± 11.5	25.6 ± 3.3	338.9 ± 21.2	94.6 ± 18.4	77.2 ± 4.9
42.4	146.2 ± 24.5	53 ± 8.4	522.9 ± 58.2	199.4 ± 38.4	131.4 ± 14.7
43.7	95.5 ± 13.2	67 ± 10.6	424.3 ± 47.3	222.3 ± 42.8	121.8 ± 13.6
44.9	80.6 ± 11.2	87.5 ± 13.9	413.5 ± 46.1	281.8 ± 54.3	131.7 ± 14.7

produced by the following possible reaction channels:

- (1) Complete fusion of ^7Li with ^{93}Nb leads to production of the ^{96}Tc through $p3n$ channel:



- (2) Complete fusion of ^7Li with ^{93}Nb leads to production of the ^{96}Tc by $d2n$ channel:

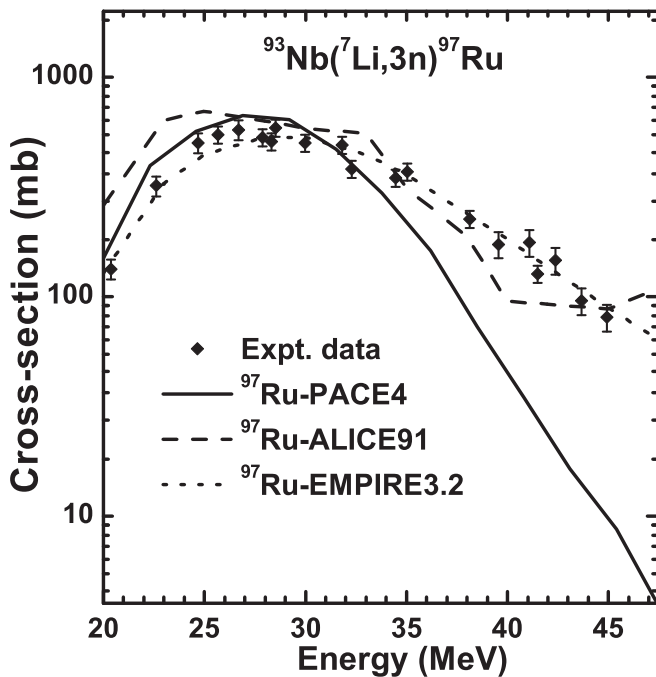
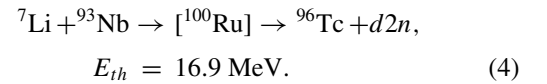


FIG. 2. Comparison of experimental (symbols) excitation functions of ^{97}Ru from the $^7\text{Li} + ^{93}\text{Nb}$ reaction and those obtained from theoretical (curves) estimation from PACE4, ALICE91, and EMPIRE3.2.

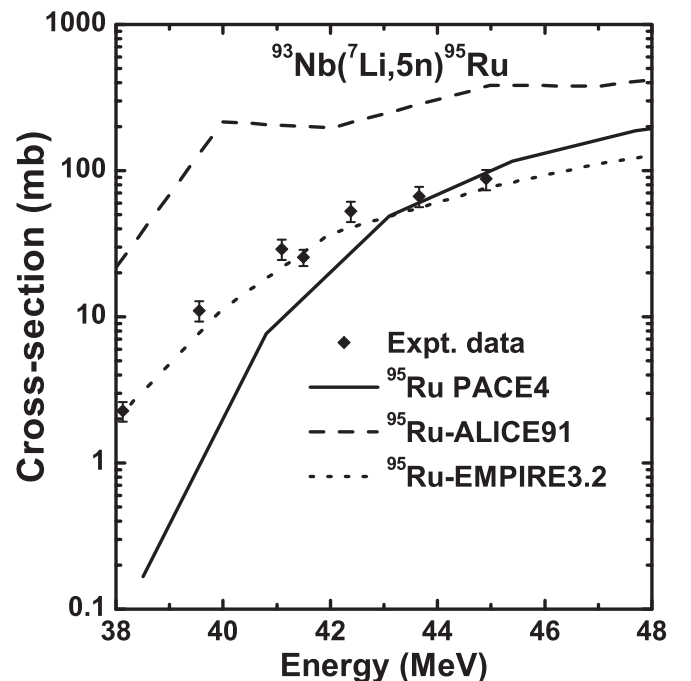


FIG. 3. Comparison of experimental (symbols) and calculated (curves) excitation functions for production of ^{95}Ru .

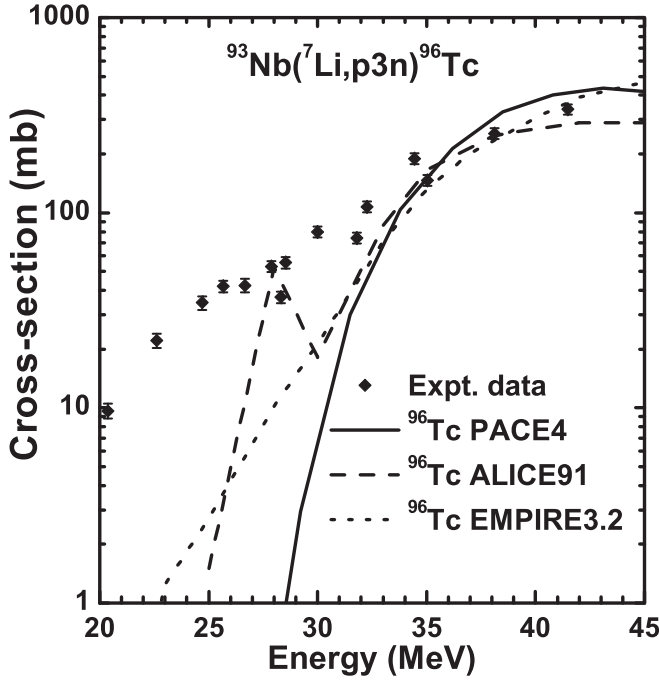


FIG. 4. Comparison of experimental (symbols) and calculated (curves) excitation functions for production of ^{96}Tc .

- (3) Complete fusion of ^7Li with ^{93}Nb leads to production of the ^{96}Tc by tn channel:

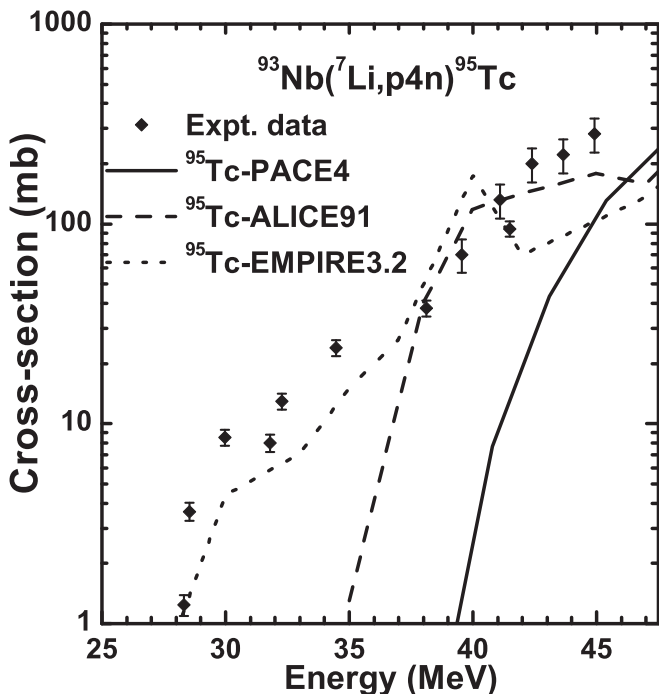
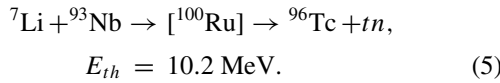


FIG. 5. Comparison of experimental (symbols) and calculated (curves) excitation functions for production of ^{95}Tc .

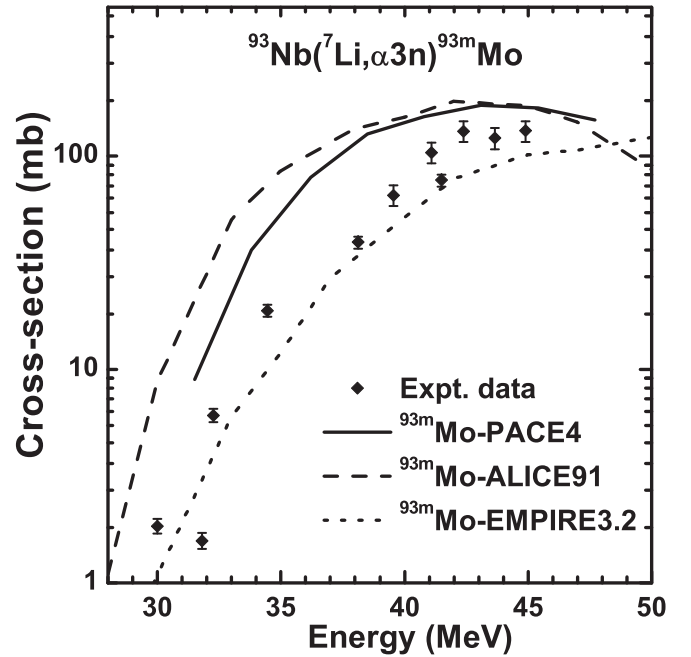
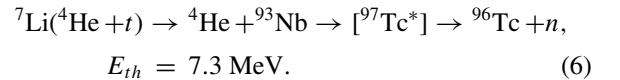
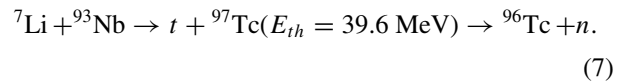


FIG. 6. Comparison of experimental (symbols) and calculated (curves) excitation functions for production of ^{93m}Mo .

- (4) It is possible that ^7Li dissociates into an α particle and tritium in the nuclear force field. The α particle, the secondary projectile, fuses with ^{93}Nb forming a composite nucleus $^{97}\text{Tc}^*$, which emits one neutron to form ^{96}Tc , and tritium moves in the forward direction as a spectator:



- (5) Interaction of ^7Li with ^{93}Nb may also lead to the production of t and ^{97}Tc in the excited level, which may emit one neutron to produce ^{96}Tc :



The excitation function for ^{95}Tc residue is plotted in Fig. 5. PACE4 calculations underpredict the experimental excitation function throughout the range. Although ALICE91 explains measured data in the higher energy region, it underpredicts in the lower energy region. However, EMPIRE3.2 calculations show a good agreement to the experimental data even at lower energies. Figure 6 shows the production of the ^{93m}Mo radionuclide. PACE4 and ALICE91 overpredict the experimental data throughout the energy region, while EMPIRE3.2 reproduced the experimental data successfully.

It is remarkable that EMPIRE3.2 calculations are in good agreement with the measured excitation functions of all the residues. It projects the effectiveness of the EMPIRE3.2 nuclear reaction code in understanding the heavy-ion induced reaction

in the low and intermediate energy range. ALICE91 was intended only to study light-ion (n , p , d , α -particle) induced reactions while the EMPIRE3.2 code is competent for both light- as well as heavy-ion induced reactions.

From the measured excitation functions, it is seen that production of neutron deficient ^{97}Ru radionuclides in the 22–35 MeV energy range is high compared to other coproduced radionuclides ^{96}Tc and ^{95}Tc , which along with bulk Nb can be chemically separated easily from the ^{97}Ru [24]. The maximum cross section (~ 580 mb) of ^{97}Ru was observed at 28.5 MeV energy along with one tenth of ^{96}Tc radioisotopes.

V. CONCLUSION

Production cross sections of all the residual radionuclides produced in the $^7\text{Li} + ^{93}\text{Nb}$ reaction have been studied in the 20–45 MeV energy range and are compared with the theoretical model calculations of PACE4, ALICE91, and EMPIRE3.2 with suitable choices of parameters. Overall, EMPIRE3.2 estimations agree well with all the measured excitation functions. Measured cross-section data indicate the compound nuclear reaction process as a predominant mechanism. However, significant PEQ emission of neutrons was also observed in the high energy tail of the excitation function in the $3n$ emission

channel. Therefore, higher values of cross-section data at the high energy tail could only be explained by the contributions of compound and PEQ processes. In order to understand the PEQ emission in the xn , $x \geq 5$ channel, experimental data are needed in the higher energy region. Further, an indirect signature of incomplete fusion was also observed in the production of the ^{96}Tc radioisotope. Since ^7Li is a weakly bound projectile, it can easily break into an α particle and tritium. It is expected that breakup fusion of the α particle might have taken place with ^{93}Nb and the subsequent emission of a neutron by a compound or PEQ process may produce ^{96}Tc . However, proper investigation of breakup fusion, such as by the recoil range distribution method, is needed for the confirmation of incomplete fusion in the $^7\text{Li} + ^{93}\text{Nb}$ system.

ACKNOWLEDGMENTS

The authors convey their sincere thanks to the Pelletron staff and target laboratory staff of the BARC-TIFR Pelletron facility for their cooperation and help during the experiment. The work is financially supported by MHRD, IITR/SRIC/218/FIG and SINP-DAE-12-plan project TULIP grant, Government of India.

-
- [1] H. C. Britt and A. R. Quinon, *Phys. Rev.* **124**, 877 (1961).
 [2] D. J. Parker, J. Asher, T. W. Conlon, and I. Naqib, *Phys. Rev. C* **30**, 143 (1984).
 [3] D. J. Parker, J. J. Hogan, and J. Asher, *Phys. Rev. C* **39**, 2256 (1989).
 [4] M. Dasgupta, D. J. Hinde, N. Rowley, and A. M. Stefanini, *Annu. Rev. Nucl. Part. Sci.* **48**, 401 (1998).
 [5] J. F. Liang and C. Signorini, *Int. J. Mod. Phys. E* **14**, 1121 (2005).
 [6] L. F. Canto, P. R. S. Gomes, R. Donangelo, and M. S. Hussein, *Phys. Rep.* **424**, 1 (2006).
 [7] N. Keeley, R. Raabe, N. Alamanos, and J. L. Sida, *Prog. Part. Nucl. Phys.* **59**, 579 (2007).
 [8] L. F. Canto, P. R. S. Gomes, R. Donangelo, J. Lubian, and M. S. Hussein, *Phys. Rep.* **596**, 1 (2015).
 [9] K. E. Rehm, H. Esbensen, C. L. Jiang, B. B. Back, F. Borasi, B. Harss, R. V. F. Janssens, V. Nanal, J. Nolen, R. C. Pardo, M. Paul, P. Reiter, R. E. Segel, A. Sonzogni, J. Uusitalo, and A. H. Wuosmaa, *Phys. Rev. Lett.* **81**, 3341 (1998).
 [10] C. Birattari, M. Bonardi, M. Cavinato, E. Fabrici, E. Gadioli, E. Gadioli Erba, F. Groppi, M. Bello, C. Bovati, A. Di Filippo, T. G. Stevens, S. H. Connell, J. P. F. Sellschop, S. J. Mills, F. M. Nortier, G. F. Steyn, and C. Marchetta, *Phys. Rev. C* **54**, 3051 (1996).
 [11] M. Cavinato, E. Fabrici, E. Gadioli, E. Gadioli Erba, P. Vergani, M. Crippa, G. Colombo, I. Redaelli, and M. Ripamonti, *Phys. Rev. C* **52**, 2577 (1995).
 [12] P. Vergani, E. Gadioli, E. Vaciano, E. Fabrici, E. Gadioli Erba, M. Galmarini, G. Ciavola, and C. Marchetta, *Phys. Rev. C* **48**, 1815 (1993).
 [13] M. Dasgupta, P. R. S. Gomes, D. J. Hinde, S. B. Moraes, R. M. Anjos, A. C. Berriman, R. D. Butt, N. Carlin, J. Lubian, C. R. Morton, J. O. Newton, and A. Szanto de Toledo, *Phys. Rev. C* **70**, 024606 (2004).
 [14] M. Dasgupta, D. J. Hinde, K. Hagino, S. B. Moraes, P. R. S. Gomes, R. M. Anjos, R. D. Butt, A. C. Berriman, N. Carlin, C. R. Morton, J. O. Newton, and A. Szanto de Toledo, *Phys. Rev. C* **66**, 041602(R) (2002).
 [15] F. Amorini, M. Cabibbo, G. Cardella, A. Di Pietro, P. Figuera, A. Musumarra, M. Papa, G. Pappalardo, F. Rizzo, and S. Tudisco, *Phys. Rev. C* **58**, 987 (1998).
 [16] M. K. Sharma, P. P. Singh, D. P. Singh, A. Yadav, V. R. Sharma, I. Bala, R. Kumar, Unnati, B. P. Singh, and R. Prasad, *Phys. Rev. C* **91**, 014603 (2015).
 [17] M. Maiti and S. Lahiri, *Phys. Rev. C* **79**, 024611 (2009).
 [18] S. C. Srivastava, P. Som, G. Meinken, A. Sewatkar, and T. H. Ku, Brookhaven National Laboratory Report No. BNL 24614 (1978).
 [19] M. C. Lagunas-Solar, M. J. Avila, N. J. Nvarro, and P. C. Johnson, *Int. J. Appl. Radiat. Isot.* **34**, 915 (1983).
 [20] N. G. Zaitseva, E. Rurarz, M. Vobecky, K. H. Hwan, K. Nowak, T. Tethal, V. A. Khalkin, and L. M. Popinenkova, *Radiochim. Acta* **56**, 59 (1992).
 [21] D. Comar and C. Crouzel, *Radiochem. Radioanal. Lett.* **27**, 307 (1976).
 [22] G. Comparetto and S. M. Qaim, *Radiochim. Acta* **27**, 177 (1980).
 [23] P. J. Pao, J. L. Zhou, D. J. Silvester, and S. L. Waters, *Radiochem. Radioanal. Lett.* **46**, 21 (1981).
 [24] M. Maiti and S. Lahiri, *Radiochim. Acta* **99**, 359 (2011).
 [25] M. Maiti and S. Lahiri, *Radiochim. Acta* **103**, 7 (2015).
 [26] M. Maiti, *Radiochim. Acta* **101**, 437 (2013).
 [27] J. F. Ziegler, M. D. Ziegler, and J. P. Biersack, *Nucl. Instrum. Methods Phys. Res., Sect. B* **268**, 1818 (2010).
 [28] M. Maiti and S. Lahiri, *Phys. Rev. C* **81**, 024603 (2010).
 [29] M. Maiti and S. Lahiri, *Phys. Rev. C* **84**, 067601 (2011).
 [30] M. Maiti, *Phys. Rev. C* **84**, 044615 (2011).
 [31] <http://www.nndc.bnl.gov/nudat2/> (National Nuclear Data Center, Brookhaven National Laboratory).

- [32] B. Wilke and T. A. Fritz, *Nucl. Instrum. Methods* **138**, 331 (1976).
- [33] J. Kemmer and R. Hofmann, *Nucl. Instrum. Methods* **176**, 543 (1980).
- [34] A. Gavron, *Phys. Rev. C* **21**, 230 (1980).
- [35] M. Blann and H. K. Vonach, *Phys. Rev. C* **28**, 1475 (1983).
- [36] M. Blann, Lawrence Livermore National Laboratory Report No. UCID 19614, 1982; M. Blann, paper SMR/284-1, in Proceedings of the International Centre for Theoretical Physics Workshop on Applied Nuclear Theory and Nuclear Model Calculations for Nuclear Technology Applications, Trieste, Italy, 1988 (unpublished).
- [37] M. Herman, R. Capote, B. V. Carlson, P. Oblozinsky, M. Sin, A. Trkov, H. Wienke, and V. Zerkin, *Nucl. Data Sheets* **108**, 2655 (2007).
- [38] R. Bass, *Phys. Rev. Lett.* **39**, 265 (1977).
- [39] C. M. Perey and F. G. Perey, *At. Data Nucl. Data Tables* **17**, 1 (1976).
- [40] M. Blann, *Phys. Rev. Lett.* **27**, 337 (1971).
- [41] V. F. Weisskopf and D. H. Ewing, *Phys. Rev.* **57**, 472 (1940).
- [42] H. Lenske and H. H. Wolter, TRISTAN and ORION codes (private communication).
- [43] M. B. Chadwick, DDHMS code (private communication).
- [44] J. Raynal, Optical-Model and Coupled-Channel Calculations in Nuclear Physics, International Atomic Energy Agency Report IAEA-SMR-9/8 (1972).
- [45] J. Raynal, in *Computing as a Language of Physics*, ICTP International Seminar Course (IAEA-ICTP, Trieste, 1972), p. 281.
- [46] C. H. Dasso and S. Landowne, *Comput. Phys. Commun.* **46**, 187 (1987).